

Neurological functional evaluation based on accurate motions in big animals with traumatic brain injury

Ji-Peng Jiang^{1, #}, Xue-Gang Niu^{2, #}, Chen Dai¹, Ke Ma¹, Hui-You Xu¹, Shi-Xiang Cheng¹, Zhi-Wen Zhang³, Feng Duan³, Xu Zhu⁴, Yu-Ting Wang⁴, Xu-Yi Chen^{1, #}, Sai Zhang^{1, #}

1 Center for Neurology and Neurosurgery, Medical Center of People's Armed Policed Force, Key Laboratory of Neurotrauma Repair of Tianjin, Tianjin, China

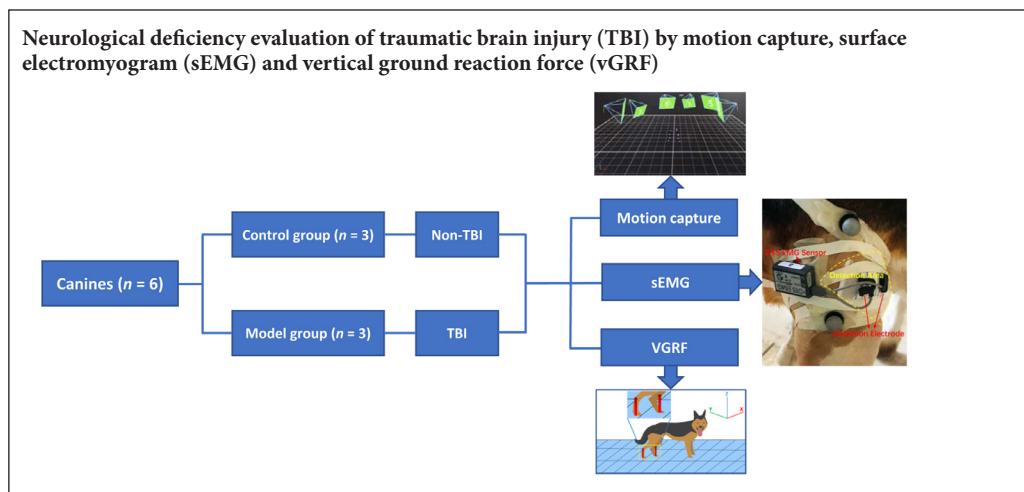
2 Department of Neurosurgery, Tianjin Fourth Central Hospital, Tianjin, China

3 Department of Automation, College of Computer and Control Engineering, Nankai University, Tianjin, China

4 Graduate School, Tianjin Medical University, Tianjin, China

Funding: This work was supported by the National Natural Science Foundation of China, No. 11672332, 11102235 and 31200809 (all to XYC); the National Key Research and Development Plan of China, No. 2016YFC1101500 (to SZ); and the Science and Technology Program of Tianjin, China, No. 17YFZCSY00620 and 16ZXHLSY00120 (both to XYC).

Graphical Abstract



*Correspondence to:

Xu-Yi Chen, MD,
chenxuyi1979@126.com;
Sai Zhang, MD,
Zhangsai718@yahoo.com.

#These authors contributed equally to this work.

orcid:

0000-0002-8954-7277
(Ji-Peng Jiang)

doi: 10.4103/1673-5374.250578

Received: May 31, 2018

Accepted: December 17, 2018

Abstract

An accurate and effective neurological evaluation is indispensable in the treatment and rehabilitation of traumatic brain injury. However, most of the existing evaluation methods in basic research and clinical practice are not objective or intuitive for assessing the neurological function of big animals, and are also difficult to use to qualify the extent of damage and recovery. In the present study, we established a big animal model of traumatic brain injury by impacting the cortical motor region of beagles. At 2 weeks after successful modeling, we detected neurological deficiencies in the animal model using a series of techniques, including three-dimensional motion capture, electromyogram and ground reaction force. These novel technologies may play an increasingly important role in the field of traumatic brain injury diagnosis and rehabilitation in the future. The experimental protocol was approved by the Animal Care and Use Committee of Logistics University of People's Armed Police Force (approval No. 2017-0006.2).

Key Words: nerve regeneration; evaluation method; neurological deficiency; traumatic brain injury; motion capture; electromyogram; ground reaction force; neural regeneration

Chinese Library Classification No. R443; R363; R741

Introduction

Traumatic brain injury (TBI) has been one of the leading causes of death and disability worldwide (Tan and Hutchinson, 2018; Kinder et al., 2019). The primary and secondary injuries tend to result in poor prognosis. Even when timely and effective post-traumatic intervention is received, survivors may be left with physical disabilities and neurological deficiencies (Henry et al., 2018; Morganti-Kossmann et al., 2018; Zibara et al., 2019).

Because of the refractory and prognostic uncertainty of

TBI, neurological functional evaluation is of extraordinary significance (Ouyang et al., 2018), especially during rehabilitation, as neurological evaluation can accurately reflect the efficacy of rehabilitation and provide direction for subsequent treatment (Brochard et al., 2010; Mumford et al., 2010). Up to now, many scoring scales have been developed and are widely used in the field of neurology. Among the scales, motor ability is a particularly important indicator that has been evaluated intensively. It determines whether an individual is able to act autonomously or have a self-heal-

ing capacity after nerve injury or nervous system disease. In basic research, many scales have been used for the neurological evaluation of rodents and mammals. As early as the 1980s, Bederson et al. (1986) and McIntosh et al. (1989) proposed the use of scoring scales to assess the motor function of rats with brain injury, which are still in use to date. In the studies addressing TBI in big animals, there are limited motor function scales. The Modified Glasgow Coma Scale (Platt et al., 2001; Beltran et al., 2014) and Purdy scoring scales (Purdy et al., 1989) have been used in some studies in canines. In clinical practice, the Fugl-Meyer scoring system may be the most classic and comprehensive scale in the field of rehabilitation, and it has been used in numerous studies including clinical trials related to motor impairment following stroke and TBI (Fugl-Meyer et al., 1975a, b; Gladstone et al., 2002). These scoring scales reflect the neurological motor status of animals or humans after TBI and other nervous system diseases. They are of certain guiding significance for basic research and clinical practice. However, the subjective consideration and personal orientation of the evaluator and the sample size may generate biases that largely restrict the effectiveness and accuracy of the evaluation.

We considered whether there are any new methods that can independently characterize the motor status of experimental subjects in an easy-to-understand way and extract accurate data to explain and verify the real-time status. Therefore, we used three-dimensional motion capture, electromyogram (EMG) and ground reaction force (GRF) based on the anatomical structure of joints and muscles, to reveal the kinematic and mechanical characteristics and related functional changes of neurological deficiencies from an assessment of motion composition overall. Up to now, similar techniques have been used in basic studies of spinal cord injury. However, these techniques have been rarely used in TBI research and clinical practice, and it would be very valuable to validate these techniques and develop similar evaluation systems for TBI.

Materials and Methods

Experimental animals

Six 1-year-old male beagles, weighing 11–14 kg, were purchased from Fang Yuanyuan Animal-Feeding Center, Beijing, China (license No. SCXK 2014-0012). They were randomly assigned into a control group ($n = 3$) or model group ($n = 3$). The experimental protocol was launched under the approval of the Animal Care and Use Committee of Logistics University of People's Armed Police Force in China (approval No. 2017-0006.2). All invasive operations in animals were performed under general anesthesia to minimize the suffering of the animals.

Establishment of TBI models

Before anesthesia, the canines were subjected to fasting for 8 hours and water deprivation for 4 hours. Then, general anesthesia was followed by intramuscular injection with pentobarbital sodium at a dose of 30 mg/kg. The canine tongue was drawn out gently and endotracheal intubation with mechanical ventilation was performed to make sure there was an adequate oxygen supply throughout the operation. Normal

saline was also administered via intravenous infusion of the hindlimb. Except for general anesthesia, the canines in the control group received no surgical interventions. In the model group, the canines were subjected to traumatic cortical motor area injury on the left side after bone window craniotomy and the dura mater was opened. The canines were first immobilized in a prone position with four limbs fixed onto the table at the functional position of the joints to avoid joint injuries or peripheral nerve and blood vessel entrapments; then, the whole area of the head was shaved and the flaps were designed along the boundaries of temporal muscle to minimize the injury on the right side. After shaving, the area of operation was sterilized with iodophor and covered with a sterile towel. A curve incision was made on the scalp, and the subcutaneous tissue was exposed. The temporal muscle was bluntly separated, and the bony window was designed with a 3.5-cm long axis, 3-cm short axis and 0.5 cm away from the midline after the removal of periosteum and hemostasis. The bony window was opened with a hand-held cranial drill (RWD Life Science Company, Shenzhen, China) and the sectional edge of the skull was sealed with bone wax to prevent bleeding. A cross-shaped incision was made on the dura mater and suspended on the bone edge. A large vein was used as a reference marker on the surface of the cerebral cortex. A standardized injury was made near the leading edge of the marked blood vessel in the right cerebral hemisphere using a modified electric Cortical Contusion Impactor (eCCI; RWD Life Science Company), with a modification on the impact probe from 2 mm to 8 mm in diameter. The parameters were set as 9.99 mm in depth, 5.34 m/s in speed and 255 ms in dwell time. After impacting, the traumatic foci were rinsed with warm normal saline and the necrotic tissue was removed carefully with a meninges detacher and tissue forceps under an operating microscope. Gelatin sponge was applied to the periphery and base of the traumatic foci to deal with bleeding thoroughly. The relaxation suture of the dura mater was performed with an artificial dura patch by using absorbable 6/0 surgical sutures and the bleeding problems were resolved with a bipolar coagulation system (GN060, AESCULAP AG & CO.KG, Tuttlingen, Germany). The scalp was sutured with the subcutaneous tissue using absorbable 4/0 surgical sutures and the wound was disinfected with iodophor.

The canines were kept at a constant temperature until recovering from anesthesia, extubated and housed in cages separately with drinking water and liquid diet available ad libitum in a soundproof room. The canines were given penicillin at a dose of 3×10^4 U/kg twice a day by intramuscular injection for 5 continuous days. Buprenorphine hydrochloride for pain relief was infused once a day for 3 consecutive days at a dose of 0.03 mg/kg.

Three-dimensional motion capture

EMG and GRF were used to evaluate the motor function 2 months post-operation, which were performed and recorded using the Vicon Motion Capture System (Oxford Metrics Limited, Oxford, UK) composed of six high-speed cameras. We adjusted the visual field of the system (**Figure 1A**) and then attached four fluorescent markers around the four major joints

(named as joints a, b, c and d) of each hindlimb. The endpoint in this study was set to measure the real-time height of the lowest point of the limb when the animal was walking (Figure 1B); real-time height of this lowest point, angle of joints b and c, and the trajectory of each joint along with the distance variation were also photographed and recorded by the cameras by capture of the markers when walking (Figure 1C). The speed of the treadmill was set at 1.5 km/h throughout the whole process.

Electromyogram

As the biceps femoris is the major muscle of the limb muscle group, we detected and recorded its real-time EMG signals. Two bipolar electrodes and an EMG sensor were attached to the shaved, cleaned and alcohol-treated skin at the middle third of the distance between the ischial tuberosity and patella of bilateral hindlimbs based on anatomical descriptions of muscle locations (Marras and Davis, 2001; Breiffuss et al., 2015; Alizadeh et al., 2016). The sampling frequency was set as 1500 Hz when walking. EMG data were collected with DTS EMG sensor system (Noraxon, Scottsdale, Arizona, USA) (Figure 2A).

Ground reaction force measurement

The detection device we used was AMTI force platform (Advanced Mechanical Technology Inc, Watertown, Massachusetts, USA). A treadmill was prepared and placed on the force platform with the canine. The initial force was zeroed at the beginning of each measurement. The step force in the direction of the Z-axis was detected as vertical GRF (vGRF) when walking.

Statistical analysis

The quantitative data, including height, amplitude and force, were recorded as the mean \pm SD. Statistical analyses were performed with the software SPSS 22.0 (IBM, Armonk, New York, USA). Independent-sample *t*-test was performed and significant differences between groups were determined as $P < 0.05$ and $P < 0.01$.

Results

Gait characteristics in the TBI beagle model

After 2 months of rehabilitation, the motor function evaluation was performed by three-dimensional motion capture. Gait analysis consisted of angle changes, distance variation and trajectory. Trajectories of the four left joints in the direction of the X-, Y- and Z-axis were normal in the control group but irregular in the model group (Figure 3A-H). Changes of the distance from the calibration point of the four left joints in the model group were irregular. Angle changes of joints b and c of the left hindlimb in the model group were irregular (Figure 3C, D, G, and H). The changes in the endpoint height of the left hindlimb in the model group were irregular and significantly lower than those of the right hindlimb (Figure 3I-K; $P < 0.05$).

Electromyogram characteristics in the TBI beagle model

The EMG detection results of the bilateral hindlimbs were

very similar in the control group (Figure 2B and C), whereas there was almost no signal of the left hindlimb in the model group (Figure 2D and E). The average voltage of the left hindlimb in the model group was significantly lower than that of the right hindlimb (Figure 2F; $P < 0.01$).

Ground reaction force characteristics in the TBI beagle model

The vGRF showed regular changes in the control group, but was irregular in the model group, especially for the left hindlimb when walking (Figure 2G). Additionally, vGRF of the left hindlimb was lower than that of the right hindlimb in the model group (Figure 2H; $P < 0.01$).

Discussion

TBI is a serious public health problem worldwide that causes death and disability, such as cognitive deficits, dysphasia, and hemiplegia (Royo et al., 2003; McConeghy et al., 2012; Shi et al., 2012). If the disease cannot be assessed effectively, patients are likely to miss the optimal therapeutic opportunity. As a complex disease, damage to motor function caused by TBI is sometimes hidden, and it is difficult to detect intrinsic neurological deficits by observing the symptoms and signs superficially.

Bones, joints, and muscles are essential components of body movement. In this study, we used the motion capture system to show the real-time motion state, particularly of the four major joints represented by a, b, c and d, which were equivalent to the toe, ankle, knee and hip joints, respectively. The main endpoint was to observe and detect the limb height in real time, reflecting the ability of the limb to work against gravity. There is evidence that central nervous system circuits may provide an explicit representation of limb endpoint kinematics (Bosco and Poppele, 2001). Moreover, neurobehavioral experiments have suggested that the limb endpoint is the primary variable used to coordinate locomotion in animal models (Courtine et al., 2005) and humans (Ivanenko et al., 2008). In addition, the lower limb endpoint is a relevant neurological variable to encode and organize movements of the lower limbs (Wenger et al., 2014). When walking, each joint has its own trajectory. Under uniform motion, the trajectory of the joint without motor deficits is regular; irregular trajectory indicates the joint is unstable. In our study, the trajectories of the four major joints of the left hindlimb in the model group were obviously irregular compared with the right hindlimb. Further, we observed the angle variations of joints b and c, and the joints of the model group showed greater variability than those of the control group. Significant differences in the stride were also found between the groups. Irregularities appeared in all measures of the left limb in the model group, reflecting abnormalities of the joint activity and the sensitivity and effectiveness of the motion capture system.

Surface EMG (sEMG), also called dynamic EMG, was used in this study, and the collection frequency we chose was based on previous related studies (Chow et al., 2012; Breiffuss et al., 2015). The variations of sEMG largely reflect the changes of muscle activity and the characteristics

of central nervous system control, such as the local fatigue degree of muscle activity, muscle strength, muscle activation mode, excitation speed of a motor unit, and multiple muscle coordination. To date, sEMG has been used in many basic research studies and clinical applications (Robert et al., 1999; Licka et al., 2004), especially in the field of TBI, stroke

and other neurological diseases, in which the assessment of neuromuscular function and rehabilitation has been a hot topic and a focus for product development. Generally speaking, compared with the classic needle EMG, which is usually used in small animals for the exact measurement of specific muscle groups (Bockstahler et al., 2009, 2012), sEMG is still in the development stage. It uses a non-invasive portable device, and sEMG recordings represent a summation of signals from the target muscles and adjacent muscles because of the “crosstalk” detection (Bockstahler et al., 2009, 2012).

GRF variations can be also detected in real time. Although it may be possible that the GRF varies between a treadmill and land, a previous study has shown that there is no significant difference in vGRF between these conditions (Drüen et al., 2010; Kluitenberg et al., 2012). Furthermore, to eliminate the measurement error caused by individual weight, we put each canine and treadmill on the force platform and zeroed the initial force for each measurement. The GRF in this study was divided into two directions including the Y- and Z-axis, and we used standard techniques to measure vGRF. The sensitivity of this method was very high, and easily identified the limb dysfunction. When neurological deficits occur, in particular once the motor-control nerve is injured, joint stability, diastole and contraction of the muscle are restricted, directly leading to limb weakness and difficulty in supporting the body weight. Even during short-term exercise, fatigue will appear early and be more obvious than in the normal condition.

Over the years, various methods have been developed to analyze locomotor function and neurological changes in

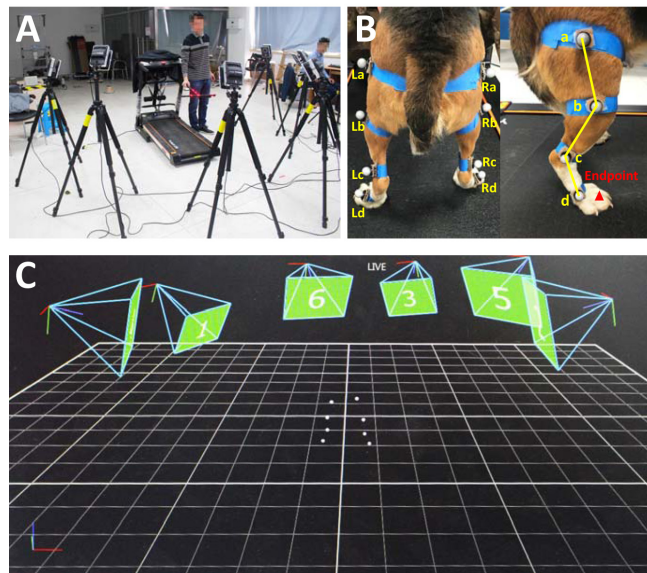


Figure 1 Construction of the motion capture platform. (A) High speed cameras were placed around the treadmill and the visual field was adjusted before motion capture. (B) Four markers were attached to each side of the hindlimbs and an endpoint (▲) was set simultaneously. L: Left hindlimb; R: right hindlimb; a-d: major joints. (C) Localization of the markers in the motion capture system. 1-6: High speed cameras 1-6.

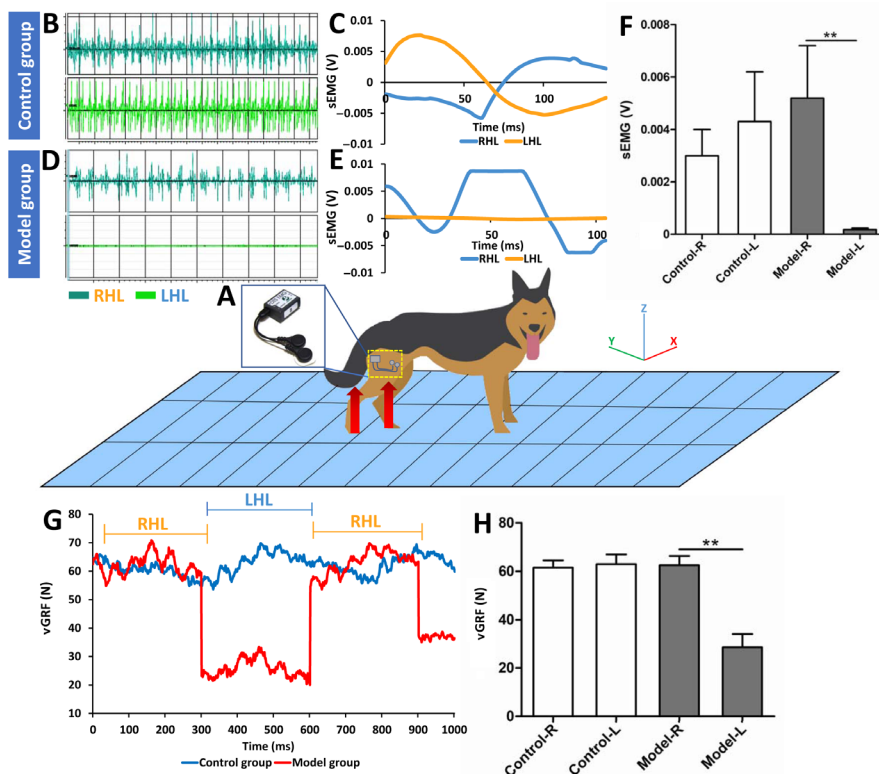


Figure 2 Surface electromyogram (sEMG) and vertical ground reaction force (vGRF) changes in the traumatic brain injury (TBI) beagle model. Damage was localized in the right cerebral cortex. (A) Schematic diagram of sEMG and vGRF detection. (B) Voltages of sEMG on bilateral hindlimbs in the control group were similar under the sampling frequency of 1500 Hz. (C) sEMG changes were regular and symmetric between the left and right hindlimb in the control group. (D) Voltage of sEMG on the right hindlimb was significantly higher than that of the left hindlimb. (E) The curve of sEMG change on the left hindlimb was almost a straight line that was asymmetrical with the right hindlimb in the model group. (F) Average sEMG voltage of the right hindlimb was significantly higher than that of the left hindlimb. (G) The curve of vGRF change was irregular in the model group and regular in the control group. (H) Average force of the right hindlimb was significantly higher than that of the left hindlimb. RHL: Right hindlimb; LHL: left hindlimb; L: left; R: right. Data in Figure 2F and H are expressed as the mean ± SD, and analyzed by independent-sample t test. ** $P < 0.01$.

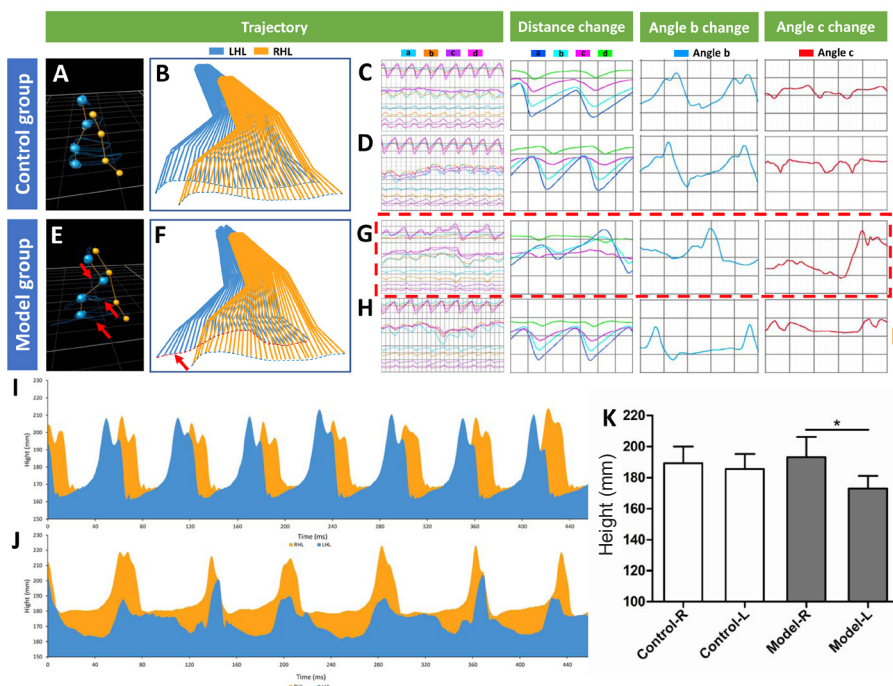


Figure 3 Gait analysis outcomes of the hindlimbs in the traumatic brain injury (TBI) beagle model.

(A) Trajectory of each joint in the control group. (B) Motion trajectories of the left and right hindlimbs were regular and symmetric in the control group. (C, D) Regular changes were found in the joint trajectory, step length and joint angles (b and c) in the control group. (E) Trajectory of each single joint was irregular in the model group. (F) Motion trajectory of the left hindlimb was irregular and asymmetrical with that of the right hindlimb in the model group. (G, H) Changes of joint trajectory in the red dotted line frame, step length and joint angles were irregular for left hindlimb and regular for the right hindlimb in the model group. (I) Height changes were regular for bilateral hindlimbs in the control group, indicated by the area diagram. (J) Height change of the left hindlimb was significantly lower than that of the right hindlimb in the model group. (K) Average height of the right hindlimb was significantly higher than that of the left hindlimb. Joint trajectory is marked by red arrows in E and F. RHL: Right hindlimb; LHL: left hindlimb; L: left; R: right. Data are expressed as the mean \pm SD, and analyzed by independent-sample *t*-test. **P* < 0.05.

small laboratory animals like rodents (Kappos et al., 2017). To gain experience with the newly developed Basso, Beattie, and Bresnahan scoring method (Basso et al., 1995), Frank Hamers developed the CatWalk gait analysis method and computer program in 1996 (van de Meent et al., 1996), which tested forelimb-hindlimb coordination in an open field (Kappos et al., 2017). Today, similar systems, such as motion capture, EMG and GRF systems, have been used in many fields. However, few of these techniques have been combined in one study to analyze the movement process comprehensively and provide insight into potential relationships between locomotion and neurological defects (Cullen et al., 2017). Similar techniques have been used in some basic and clinical studies in recent years. For example, Grégoire Courtine and colleagues have applied these methods in their research concerning spinal cord injury and have demonstrated the advanced features of these techniques (Wenger et al., 2014; Capogrosso et al., 2016). Other uses have also emerged in basic research, clinical diagnosis, rehabilitation engineering, sports medicine, geriatrics and other fields.

Traditional scoring scales of neurological evaluation no longer meet the requirements of modern research and needs of clinical practice (Neckel et al., 2018). Also, various kinds of scoring scales have been applied in experimental studies and clinical assessments. However, different experimenters or clinicians may achieve different scoring results that could lead to radically different treatment directions. Thus, it is necessary to develop accurate and objective methods to meet these needs (Jiang et al., 2018). There are some limitations of the present study. Limited samples may affect the results, and larger sample sizes will be beneficial for instrument parameter adjustment. Apart from experimental studies, specific pa-

rameters will be needed for this system to be used in clinical practice. Moreover, the results may be more convincing if the observation time had been prolonged; this will be necessary to study for translation of the system to clinical practice, as subtle changes in kinematic state can appear over time in patients, especially in those with a long disease course. Additionally, although we have demonstrated that small skull defects or defects located under the temporal muscle and occipital muscle have no adverse effects on neurologic manifestations in our previous experiments (Jiang et al., 2018), the present study did not include a sham-operated control group, which would rule out any underlying effects of the craniotomy and dura incision; this will be addressed in future studies. These techniques have great potential as a guide to assess the efficacy of TBI treatment and rehabilitation.

Acknowledgments: The authors are grateful to Jin-Long Shi from the Department of Automation, College of Computer and Control Engineering, Nankai University for his generous help during the experimental process of motion capture.

Author contributions: Study design: JPJ, XYC, SXC, FD, SZ; experiment implementation: JPJ, CD, XGN, XYC, ZWZ, XZ, KM, HXY; data analysis: YTW; material contribution and equipment coordination: SZ, XYC, FD, SXC; paper writing: JPJ. All authors approved the final version of this paper.

Conflicts of interest: The authors declare that they have no competing interests.

Financial support: This work was supported by the National Natural Science Foundation of China, No. 11672332, 11102235 and 31200809 (all to XYC); the National Key Research and Development Plan of China, No. 2016YFC1101500 (to SZ); and the Science and Technology Program of Tianjin, China, No. 17YFZCSY00620 and 16ZXHLSY00120 (both to XYC). The funding sources had no role in study design, conception, analysis or interpretation of data, writing and deciding to submit this paper for publication.

Institutional review board statement: The experimental protocol was approved by the Animal Care and Use Committee of Logistics University of People's Armed Police Force (approval No. 2017-0006.2).

Copyright license agreement: The Copyright License Agreement has been signed by all authors before publication.

Data sharing statement: Datasets analyzed during the current study are available from the corresponding author on reasonable request.

Plagiarism check: Checked twice by iThenticate.

Peer review: Externally peer reviewed.

Open access statement: This is an open access journal, and articles are distributed under the terms of the Creative Commons Attribution-NonCommercial-ShareAlike 4.0 License, which allows others to remix, tweak, and build upon the work non-commercially, as long as appropriate credit is given and the new creations are licensed under the identical terms.

References

- Alizadeh M, Zindl C, Allen MJ, Knapik GG, Fitzpatrick N, Marras WS (2016) MRI cross sectional atlas of normal canine cervical musculoskeletal structure. *Res Vet Sci* 109:94-100.
- Basso DM, Beattie MS, Bresnahan JC (1995) A sensitive and reliable locomotor rating scale for open field testing in rats. *J Neurotrauma* 12:1-21.
- Bederson JB, Pitts LH, Tsuji M, Nishimura MC, Davis RL, Bartkowski H (1986) Rat middle cerebral artery occlusion: evaluation of the model and development of a neurologic examination. *Stroke* 17:472-476.
- Beltran E, Platt SR, McConnell JF, Dennis R, Keys DA, De Risio L (2014) Prognostic value of early magnetic resonance imaging in dogs after traumatic brain injury: 50 cases. *J Vet Intern Med* 28:1256-1262.
- Bockstahler B, Kräutler C, Holler P, Kotschwar A, Vobornik A, Peham C (2012) Pelvic limb kinematics and surface electromyography of the vastus lateralis, biceps femoris, and gluteus medius muscle in dogs with hip osteoarthritis. *Vet Surg* 41:54-62.
- Bockstahler BB, Gesky R, Mueller M, Thalhammer JG, Peham C, Podbregar I (2009) Correlation of surface electromyography of the vastus lateralis muscle in dogs at a walk with joint kinematics and ground reaction forces. *Vet Surg* 38:754-761.
- Bosco G, Poppele RE (2001) Proprioception from a spinocerebellar perspective. *Physiol Rev* 81:539-568.
- Breitfuss K, Franz M, Peham C, Bockstahler B (2015) Surface electromyography of the vastus lateralis, biceps femoris, and gluteus medius muscle in sound dogs during walking and specific physiotherapeutic exercises. *Vet Surg* 44:588-595.
- Brochard S, Robertson J, Medee B, Remy-Neris O (2010) What's new in new technologies for upper extremity rehabilitation? *Curr Opin Neurol* 23:683-687.
- Capogrosso M, Milekovic T, Borton D, Wagner F, Moraud EM, Mignardot JB, Buse N, Gandar J, Barraud Q, Xing D, Rey E, Duis S, Jianzhong Y, Ko WK, Li Q, Detemple P, Denison T, Micera S, Bezaud E, Bloch J, et al. (2016) A brain-spine interface alleviating gait deficits after spinal cord injury in primates. *Nature* 539:284-288.
- Chow JW, Yablon SA, Stokic DS (2012) Electromyogram-lengthening velocity relation in plantar flexors during stance phase of gait in patients with hypertononia after acquired brain injury. *Arch Phys Med Rehabil* 93:2287-2294.
- Courtine G, Roy RR, Hodgson J, McKay H, Raven J, Zhong H, Yang H, Tuszynski MH, Edgerton VR (2005) Kinematic and EMG determinants in quadrupedal locomotion of a non-human primate (Rhesus). *J Neurophysiol* 93:3127-3145.
- Cullen KL, Dickey JP, Brown SH, Nykamp SG, Bent LR, Thomason JJ, Moens NM (2017) The magnitude of muscular activation of four canine forelimb muscles in dogs performing two agility-specific tasks. *BMC Vet Res* 13:68.
- Drüen S, Boddeker J, Nolte I, Wefstaedt P (2010) Ground reaction forces of the canine hindlimb: are there differences between gait on treadmill and force plate? *Berl Munch Tierarztl Wochenschr* 123:339-345.
- Fugl-Meyer AR, Jääskö L, Norlin V (1975a) The post-stroke hemiplegic patient. II. Incidence, mortality, and vocational return in Goteborg, Sweden with a review of the literature. *Scand J Rehabil Med* 7:73-83.
- Fugl-Meyer AR, Jääskö L, Leyman I, Olsson S, Steglind S (1975b) The post-stroke hemiplegic patient. 1. a method for evaluation of physical performance. *Scand J Rehabil Med* 7:13-31.
- Gladstone DJ, Danells CJ, Black SE (2002) The fugl-meyer assessment of motor recovery after stroke: a critical review of its measurement properties. *Neurorehabil Neural Repair* 16:232-240.
- Henry RJ, Doran SJ, Barrett JP, Meadows VE, Sabirzhanov B, Stoica BA, Loane DJ, Faden AI (2018) Inhibition of miR-155 limits neuroinflammation and improves functional recovery after experimental traumatic brain injury in mice. *Neurotherapeutics* doi: 10.1007/s13311-018-0665-9.
- Ivanenko YP, d'Avella A, Poppele RE, Lacquaniti F (2008) On the origin of planar covariation of elevation angles during human locomotion. *J Neurophysiol* 99:1890-1898.
- Jiang J, Dai C, Niu X, Sun H, Cheng S, Zhang Z, Zhu X, Wang Y, Zhang T, Duan F, Chen X, Zhang S (2018) Establishment of a precise novel brain trauma model in a large animal based on injury of the cerebral motor cortex. *J Neurosci Methods* 307:95-105.
- Kappos EA, Sieber PK, Engels PE, Mariolo AV, D'Arpa S, Schaefer DJ, Kalbermatten DF (2017) Validity and reliability of the CatWalk system as a static and dynamic gait analysis tool for the assessment of functional nerve recovery in small animal models. *Brain Behav* 7:e00723.
- Kinder HA, Baker EW, West FD (2019) The pig as a preclinical traumatic brain injury model: current models, functional outcome measures, and translational detection strategies. *Neural Regen Res* 14:413-424.
- Kluitenberg B, Bredeweg SW, Zijlstra S, Zijlstra W, Buist I (2012) Comparison of vertical ground reaction forces during overground and treadmill running. A validation study. *BMC Musculoskelet Disord* 13:235.
- Licka TF, Peham C, Frey A (2004) Electromyographic activity of the longissimus dorsi muscles in horses during trotting on a treadmill. *Am J Vet Res* 65:155-158.
- Marras WS, Davis KG (2001) A non-MVC EMG normalization technique for the trunk musculature: Part 1. Method development. *J Electromyogr Kinesiol* 11:1-9.
- McConeghy KW, Hatton J, Hughes L, Cook AM (2012) A review of neuroprotection pharmacology and therapies in patients with acute traumatic brain injury. *CNS Drugs* 26:613-636.
- McIntosh TK, Vink R, Noble L, Yamakami I, Fernyak S, Soares H, Faden AL (1989) Traumatic brain injury in the rat: characterization of a lateral fluid-percussion model. *Neuroscience* 28:233-244.
- Morganti-Kossmann MC, Semple BD, Hellewell SC, Bye N, Ziebell JM (2018) The complexity of neuroinflammation consequent to traumatic brain injury: from research evidence to potential treatments. *Acta Neuropathol* doi: 10.1007/s00401-018-1944-6.
- Mumford N, Duckworth J, Thomas PR, Shum D, Williams G, Wilson PH (2010) Upper limb virtual rehabilitation for traumatic brain injury: initial evaluation of the elements system. *Brain Inj* 24:780-791.
- Neckel ND, Dai HN, Burns MP (2018) A novel multidimensional analysis of rodent gait reveals the compensation strategies employed during spontaneous recovery from spinal cord and traumatic brain injury. *J Neurotrauma*.
- Ouyang W, Wu W, Fan Z, Wang J, Pan H, Yang W (2018) Modified device for fluid percussion injury in rodents. *J Neurosci Res* 96:1412-1429.
- Platt SR, Radaelli ST, McDonnell JJ (2001) The prognostic value of the modified Glasgow Coma Scale in head trauma in dogs. *J Vet Intern Med* 15:581-584.
- Purdy PD, Devous MD, Sr., Batjer HH, White CL, 3rd, Meyer Y, Samson DS (1989) Microfibrillar collagen model of canine cerebral infarction. *Stroke* 20:1361-1367.
- Robert C, Valette JP, Degueurce C, Denoix JM (1999) Correlation between surface electromyography and kinematics of the hindlimb of horses at trot on a treadmill. *Cells Tissues Organs* 165:113-122.
- Royo NC, Shimizu S, Schouten JW, Stover JF, McIntosh TK (2003) Pharmacology of traumatic brain injury. *Curr Opin Pharmacol* 3:27-32.
- Shi W, Nie D, Jin G, Chen W, Xia L, Wu X, Su X, Xu X, Ni L, Zhang X, Zhang X, Chen J (2012) BDNF blended chitosan scaffolds for human umbilical cord MSC transplants in traumatic brain injury therapy. *Biomaterials* 33:3119-3126.
- Tan CL, Hutchinson PJ (2018) A neurosurgical approach to traumatic brain injury and post-traumatic hypopituitarism. *Pituitary* doi: 10.1007/s11102-018-0925-z.
- van de Meent H, Hamers FP, Lankhorst AJ, Buise MP, Joosten EA, Gispen WH (1996) New assessment techniques for evaluation of posttraumatic spinal cord function in the rat. *J Neurotrauma* 13:741-754.
- Wenger N, Moraud EM, Raspovic S, Bonizzato M, DiGiovanna J, Musienko P, Morari M, Micera S, Courtine G (2014) Closed-loop neuro-modulation of spinal sensorimotor circuits controls refined locomotion after complete spinal cord injury. *Sci Transl Med* 6:255ra133.
- Zibara K, Ballout N, Mondello S, Karnib N, Ramadan N, Omais S, Nabbouh A, Caliz D, Clavijo A, Hu Z, Ghanem N, Gajavelli S, Kobeissy F (2019) Combination of drug and stem cells neurotherapy: Potential interventions in neurotrauma and traumatic brain injury. *Neuropharmacology* 145:177-198.

C-Editor: Zhao M; S-Editors: Yu J, Li CH;

L-Editors: McCollum L, Wang L, Song LP; T-Editor: Liu XL